Cell Reports

Report

Enhanced Rate of Acquisition of Point Mutations in Mouse Intestinal Adenomas Compared to Normal Tissue

Graphical Abstract

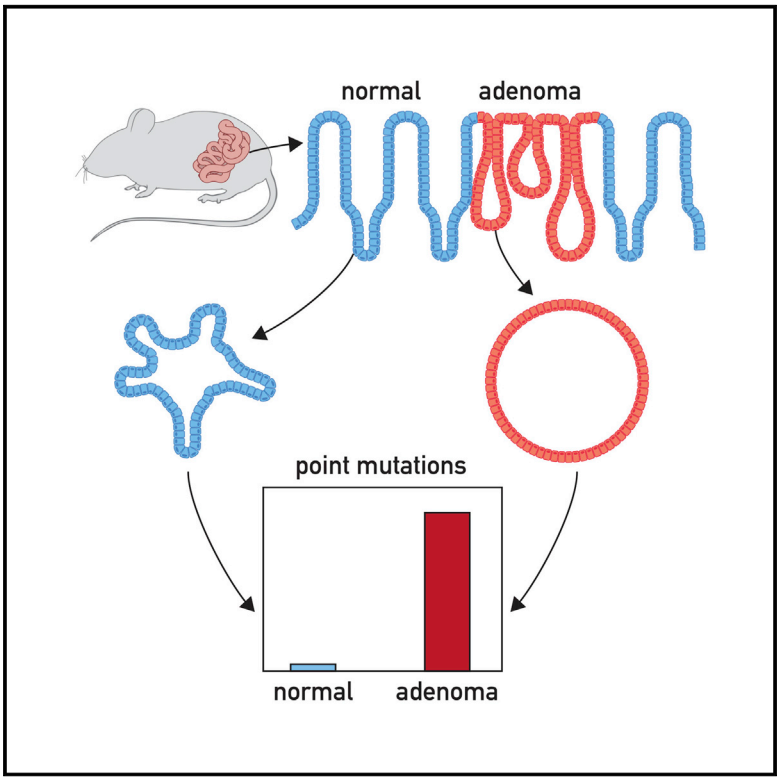

Authors

Natalia Lugli, Vasilis S. Dionellis, Paloma Ordóñez-Morán, Irene Kamileri, Sotirios K. Sotiriou, Joerg Huelsken, Thanos D. Halazonetis

Correspondence

joerg.huelsken@epfl.ch (J.H.), thanos.halazonetis@unige.ch (T.D.H.)

In Brief

By performing exome sequencing on organoids derived from single intestinal crypts from *Apc*$^{min/+}$ mice, Lugli et al. find that the rate of acquisition of point mutations in vivo increases upon transformation of normal cells to precancerous cells.

Highlights

- Exome sequencing of organoids derived from single crypts of *Apc*$^{min/+}$ mice
- The point mutation acquisition rate is ~11× higher in precancerous than in normal cells
- Loss of heterozygosity targets the wild-type *Apc* allele early in adenoma development

Lugli et al., 2017, Cell Reports *19*, 2185–2192
June 13, 2017 © 2017 The Author(s).
http://dx.doi.org/10.1016/j.celrep.2017.05.051

CellPress

Cell Reports
Report

OPEN ACCESS
CellPress

Enhanced Rate of Acquisition of Point Mutations in Mouse Intestinal Adenomas Compared to Normal Tissue

Natalia Lugli,[1,4] Vasilis S. Dionellis,[1,2,4] Paloma Ordóñez-Morán,[3,4] Irene Kamileri,[1] Sotirios K. Sotiriou,[1] Joerg Huelsken,[3,*] and Thanos D. Halazonetis[1,2,5,*]
[1]Department of Molecular Biology, University of Geneva, 1211 Geneva, Switzerland
[2]Biomedical Research Foundation of the Academy of Athens, 11527 Athens, Greece
[3]Cancer Stem Cell Laboratory, Swiss Institute of Technology Lausanne (EPFL), ISREC, 1015 Lausanne, Switzerland
[4]These authors contributed equally
[5]Lead Contact
*Correspondence: joerg.huelsken@epfl.ch (J.H.), thanos.halazonetis@unige.ch (T.D.H.)
http://dx.doi.org/10.1016/j.celrep.2017.05.051

SUMMARY

The most prevalent single-nucleotide substitution (SNS) found in cancers is a C-to-T substitution in the CpG motif. It has been proposed that many of these SNSs arise during organismal aging, prior to transformation of a normal cell into a precancerous/cancer cell. Here, we isolated single intestinal crypts derived from normal tissue or from adenomas of *Apc*$^{min/+}$ mice, expanded them minimally in vitro as organoids, and performed exome sequencing to identify point mutations that had been acquired in vivo at the single-cell level. SNSs, most of them being CpG-to-TpG substitutions, were at least ten times more frequent in adenoma than normal cells. Thus, contrary to the view that substitutions of this type are present due to normal-cell aging, the acquisition of point mutations increases upon transformation of a normal intestinal cell into a precancerous cell.

INTRODUCTION

Genomic instability is a cancer hallmark that fuels both the progression of the disease and resistance to therapy (Burrell and Swanton, 2014; Negrini et al., 2010). The term "genomic instability" comprises single-nucleotide substitutions (SNSs), small insertions and deletions (indels), microsatellite instability (MSI), copy number alterations (CNAs), and chromosomal instability (CIN). In recent years, our understanding of the mechanisms that induce genomic instability has rapidly progressed. For instance, mutations in mismatch repair (MMR) genes and DNA replication stress can lead to MSI and CIN, respectively (Burrell et al., 2013; Fishel et al., 1993). Despite this progress, the origins of point mutations in non-hereditary human cancers remain less clear. Point mutations identified in human cancers have been assigned to groups with specific mutational signatures. The most prevalent signature (signature 1) comprises C-to-T substitutions in the context of CpG motifs (Alexandrov et al., 2013). In this context, deamination of a methylated cytosine gives rise to a thymine. It has been proposed that the majority of signature 1 point mutations in cancers arise during normal aging, prior to tumor initiation (Alexandrov et al., 2013; Tomasetti et al., 2013; Tomasetti and Vogelstein, 2015; Vogelstein et al., 2013). However, in a previous study of ours, the number of point mutations in human colon adenomas did not correlate with patient age but rather with tumor size, arguing that most SNSs in these precancerous lesions accumulate after the onset of cellular transformation (Nikolaev et al., 2012). These findings are consistent with the previously proposed mutator phenotype hypothesis, which posits that the point mutation acquisition frequency increases upon transformation of a normal cell into a precancerous/cancer cell (Bielas et al., 2006; Loeb, 2011). Here, we set out to further explore the origins of point mutations in cancer.

Studies on human cancers and on mouse cancer models have been used to gain insights into cancer development (Gaspar et al., 2008; Nassar et al., 2015; Stratton, 2011). However, in most cancer sequencing studies, the DNA being sequenced is derived from many cancer cells, typically in the order of millions of cells. This means that, effectively, only mutations that are present in the majority of the cells of a tumor can be identified. However, mutations arise in single cells, and they will become detectable only if the cell in which they arose has a selective advantage and overtakes the tumor. Thus, to understand cancer development and evolution, it is necessary to sequence the genomes of single cells (Gerlinger et al., 2012).

Currently, single-cell genome sequencing is technically very challenging. To overcome this challenge, we isolated single crypts from morphologically normal intestine and from intestinal adenomas present in *Apc*$^{min/+}$ cancer-prone mice (Moser et al., 1990, 1992, 1995; Halberg et al., 2000; Yamada and Mori, 2007; Barker et al., 2009; Drost et al., 2015). These mice have a protein-coding truncating mutation in one of the *Apc* alleles. Intestinal cells that maintain the wild-type allele are normal, whereas sporadic loss of the wild-type allele results in transformation of these cells into adenomas that resemble, in every aspect, the precancerous adenomas present in human patients (Fearon, 2011). Normal and adenomatous single-crypt cells isolated from the

This is an open access article under the CC BY-NC-ND license (http://creativecommons.org/licenses/by-nc-nd/4.0/).

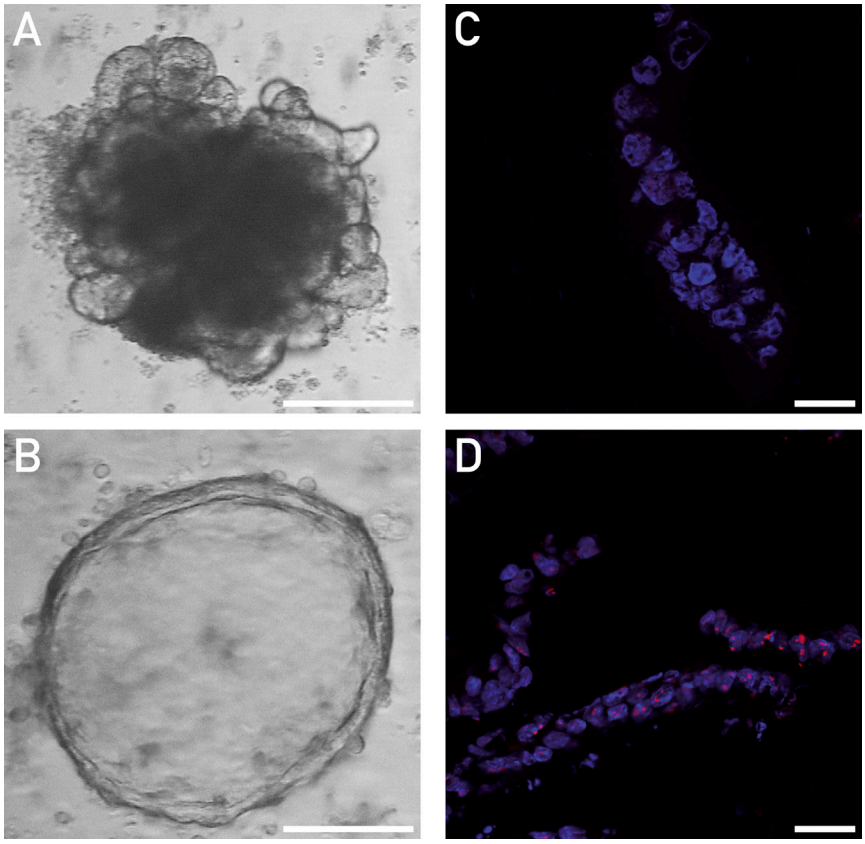

Figure 1. Growth of Small Intestine Single-Cell-Derived Organoids

(A and B) Phase-contrast images of small intestine normal (A) and tumor-derived (B) organoids. Scale bars, 200 μm.

(C and D) Immunofluorescence staining for γH2AX (red) in small intestine normal (C) and tumor-derived (D) organoids. Scale bars, 20 μm. Nuclei were counterstained with DAPI (blue).

same animal were expanded through a 3D-organoid culture system, and their exomes were sequenced.

Analysis of the sequencing data revealed that the adenoma-derived cells had, on average, almost 11 times more SNSs in the protein coding genic regions than the normal cells. Most of the SNSs were unique to each organoid, even for organoids that were derived from the same tumor. These results indicate that point mutations in mouse intestinal adenomas—and, hence, in cancers derived from these adenomas—arise after transformation of a normal cell into a precancerous cell and are, thus, in their majority, not due to normal aging.

RESULTS

Organoid Cultures from Single Normal and Transformed Small Intestinal Crypts

Since sequencing of genomic DNA from single cells cannot yet provide complete genome coverage and high sequence accuracy, we relied on ex vivo intestinal organoid cultures (Sato et al., 2009), which can be expanded in vitro, to obtain sufficient material for high-throughput sequencing (Behjati et al., 2014; Blokzijl et al., 2016). Specifically, 4-month-old $Apc^{min/+}$ mice were sacrificed, the small intestine was isolated, and single crypts were prepared from intestinal segments with macroscopically normal morphology or harboring visible adenomas. Each isolated single crypt was then expanded independently of the others as a three-dimensional culture in Matrigel. Crypts derived from the normal epithelium adopted a morphology typical of the normal small intestine, with crypt-like projections emanating from the body of the organoid (Figure 1A), whereas the organoids derived from the transformed crypts grew as spheroids and lacked crypt-like projections (Figure 1B). To simplify the terminology, we will refer to the former organoids as normal organoids and to the latter as tumor-derived organoids.

Growth of the normal organoids was dependent on the presence of R-spondin 1 and noggin in the media, which are needed for activation of the Wnt and suppression of the transforming growth factor β (TGF-β) pathways, respectively; on the contrary, proliferation of the tumor-derived organoids was independent of both R-spondin 1 and noggin, as expected (data not shown) (Sato et al., 2011). We anticipated that the normal and tumor-derived organoids would be monoclonal or, in the worst case, oligoclonal, consistent with the presence of a monoclonal stem cell population in the majority of intestinal crypts (Schepers et al., 2012).

To examine for the presence of a DNA-damage response in the organoids, we performed immunofluorescence staining for phosphorylated histone H2AX (γH2AX). The organoids derived from the macroscopically normal epithelium did not stain positive for γH2AX (Figure 1C), whereas the tumor spheroids were positive for γH2AX (Figure 1D). This staining pattern recapitulates the staining of human intestinal epithelium, where intestinal segments with normal morphology are γH2AX negative and dysplastic adenomas are γH2AX positive (Bartkova et al., 2006). Thus, these results are consistent with our model of oncogene-induced DNA replication stress, which posits that cellular transformation due to loss of tumor suppressor genes, such as *APC*, or activation of oncogenes leads to DNA replication stress and DNA damage (Halazonetis et al., 2008).

SNSs

As a first step toward comparing the patterns of genomic instability in the normal and transformed intestinal stem cells, we monitored the frequency and type of SNSs present in the exomes of normal and tumor-derived organoids. We assumed that SNSs that were acquired in vivo would be present in all cells of the organoid and, hence, should have allele frequencies

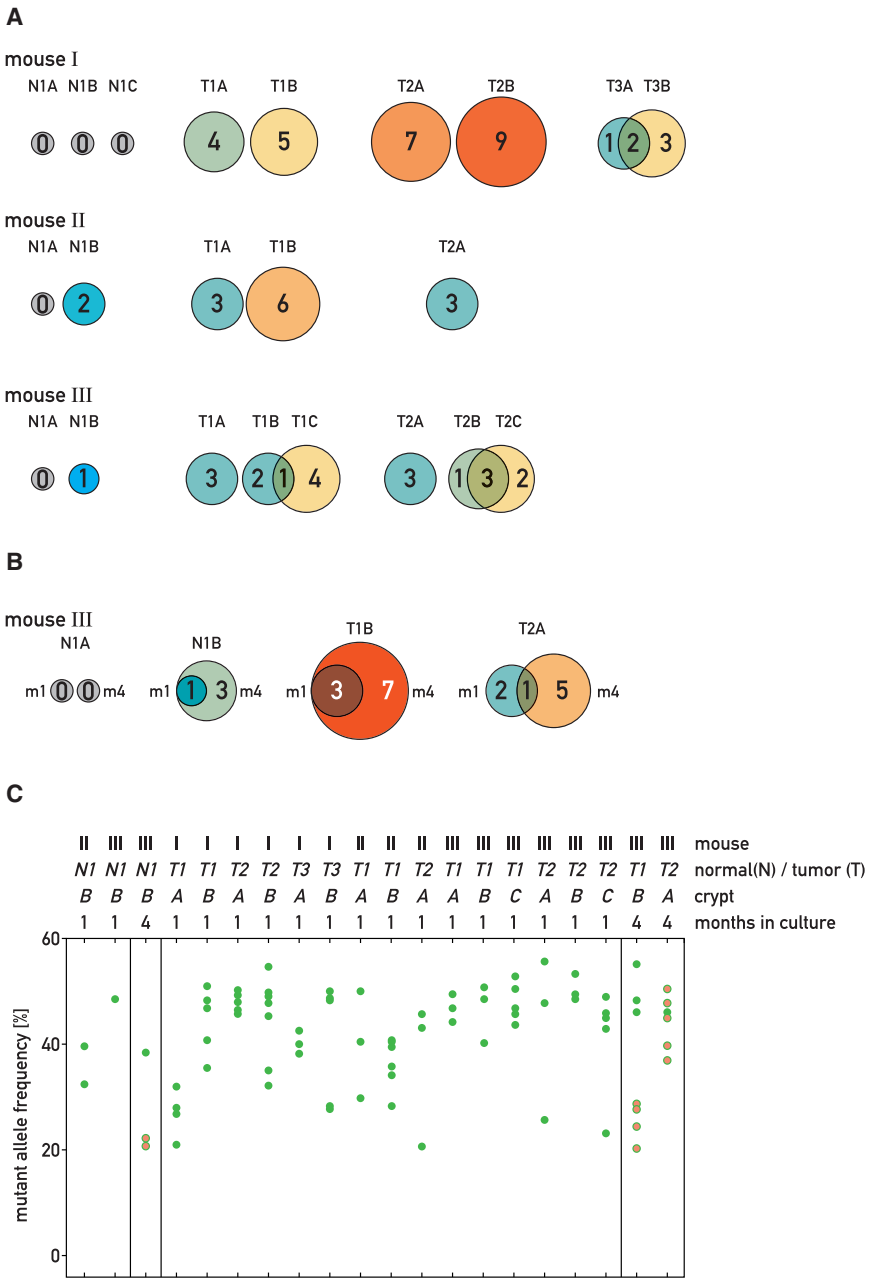

Figure 2. SNSs in Normal and Tumor-Derived Organoids

(A) Number of SNSs in 7 normal (N) and 15 tumor-derived (T) organoids from three *Apc*$^{min/+}$ mice after 1 month in culture. Distinct tumors are labeled T1, T2, etc., and crypts from these tumors are labeled A, B, etc. Mice are labeled by roman numerals. Overlaps indicate the number of shared SNSs.

(B) Number of SNSs in two normal (N) and two tumor-derived (T) organoids after 1 and 4 months (m1 and m4, respectively) in tissue culture. Overlaps indicate the number of shared SNSs.

(C) Allele frequencies of the SNSs. Green or orange dots depict SNSs detected after 1 or 4 months of in vitro culture, respectively.

of about 50% (assuming heterozygosity and monoclonal crypts). In contrast, SNSs acquired during cell culture would have much lower allele frequencies. To minimize false-positive calls, we sequenced only the exomes, as this allowed us to obtain a much higher read coverage than what would have been possible with whole-genome sequencing (Table S1). In addition, because the annotation of the mouse genome is much more accurate for coding regions than for non-coding and intergenic regions, we focused only on SNSs present within protein coding regions, as this made it easier to evaluate sequence changes identified between the normal and tumor-derived organoids.

Analysis of a total of 7 normal organoids and 15 tumor-derived organoids from three *Apc*$^{min/+}$ mice revealed a total of 71 SNSs in the protein coding regions of the genome (Table S2). The frequency of SNSs in the normal organoids was uniformly low, ranging from zero to two SNSs per organoid, with an average of 0.43 SNSs per organoid. In contrast, in the tumor-derived organoids, the number of SNSs ranged from three to nine per organoid, with an average frequency of 4.53 SNSs per organoid, which is almost 11 times higher than the frequency of SNSs in the normal organoids (Figure 2A; $p < 5 \times 10^{-8}$). None of the SNSs was shared between normal organoids derived from the same mouse, consistent with the SNSs being acquired independently of each other after development. Also, as expected, none of the SNSs was shared between organoids derived from different tumors. Remarkably, however, even in organoids derived from the same tumor, very few SNSs were shared; of the 68 SNSs present in the 15 tumor-derived organoids, 56 were found in only one organoid. The remaining 12 SNSs were each identified two times, in two different organoids derived from the same tumor (Figure 2A). From this distribution of SNSs, we infer that the vast majority of SNSs in the tumors were acquired after the cell of origin of the tumor had become transformed. Interestingly, the frequency of SNSs identified in more than one tumor-derived organoid was 0.8 SNSs per organoid, which is close to the frequency of SNSs observed in the normal organoids. Thus, these shared SNSs may have been acquired prior to cellular transformation.

All the SNSs described above had allele frequencies greater than 20%. The average allele frequency was 42.7%, as expected if SNSs were acquired in the organism rather than during expansion of the organoids in vitro (Figure 2C). In terms of their effect

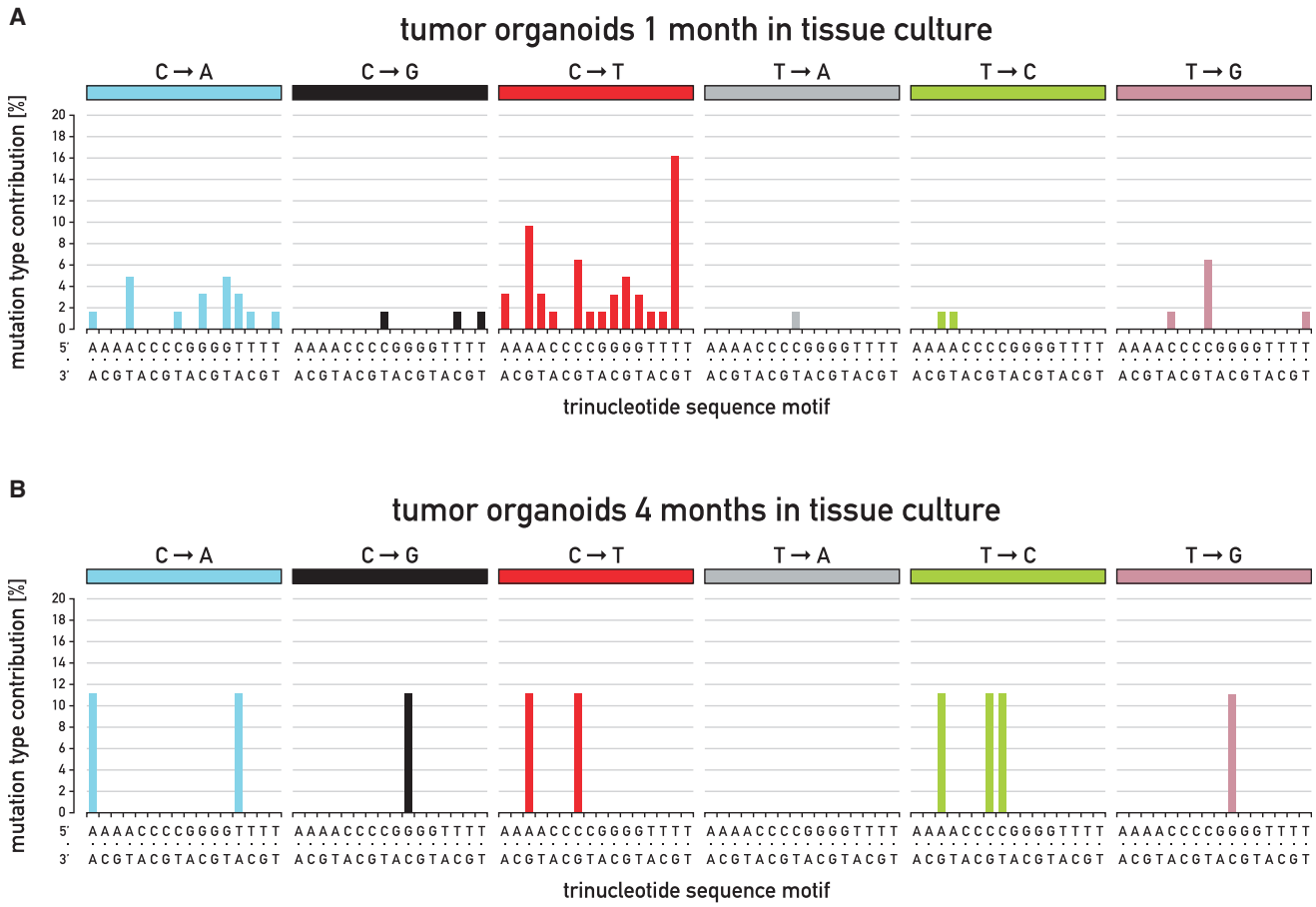

Figure 3. Mutational Signatures

(A and B) Mutational signatures of normal (N) and tumor-derived (T) small-intestine organoids after 1 month (A) or 4 months (B) in culture.

on the protein coding sequence, 55 of the SNSs identified in the tumor-derived organoids were missense mutations, 1 was a nonsense mutation, 1 was a splice-site mutation, and 11 were silent mutations. Except for the silent mutations, all the other SNSs have the potential to affect gene function. Nevertheless, none of the acquired SNSs mapped within cancer-driver genes; thus, in regard to cancer development, the identified SNSs would be classified as passenger mutations.

To monitor whether SNSs could be acquired in vitro and to assess their frequency, we continued the culture of two normal and two tumor-derived organoids for an additional 3 months and prepared genomic DNA for exome sequencing. Comparison of the SNSs identified after 1 and 4 months of culture ex vivo revealed few differences in the normal organoids; one SNS was present in the two normal organoids (III-N1A and III-N1B) after 1 month in culture; after 4 months in culture, the same SNS and two additional SNSs were observed (Figure 2B). This corresponds to an acquisition of 0.33 SNSs per organoid per month in culture. In the two tumor-derived organoids (III-T1B and III-T2A), six SNSs were identified after 1 month in culture; of these, four were also identified after 4 months in culture, and nine new SNSs were acquired. In total, 1.5 SNSs were acquired per organoid per month in culture, which is not insignificant and statistically increased compared to the normal organoids ($p < 0.033$). The SNSs observed only at the 4-month time point had generally low allele frequencies, consistent with these SNSs having been acquired in vitro (Figure 2C). Specifically, the average allele frequency of these SNSs was 33.0%, compared to 42.7% for the SNSs detected after 1 month in culture.

The most common SNS signature in human colorectal cancers and aging normal human colon cells comprises C-to-T transitions, often in the context of CpG dinucleotides (The Cancer Genome Atlas Network, 2012; Sjöblom et al., 2006). The SNSs identified in the normal and tumor-derived organoids after 1 month in culture also exhibited this signature (Figure 3A). The signature of the SNSs acquired during extended culture in vitro (4 months) appeared to be different, with no specific signature being over-represented (Figure 3B). Overall, we conclude that C-to-T transitions within CpG dinucleotides are the most common type of alteration (38% of all SNSs) in murine intestinal tumors, similar to the results obtained in human colorectal cancer patients.

CNAs

The number of sequencing reads across the genome can be used to identify CNAs. With exome data, this analysis is limited to events that involve relatively large genomic regions, since

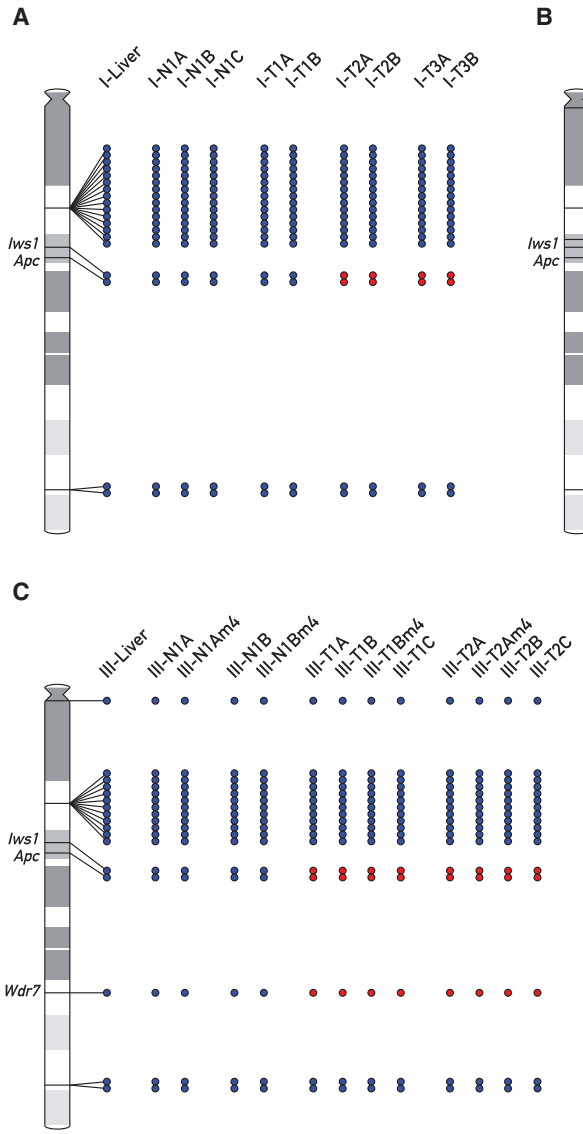

Figure 4. LOH in Normal and Tumor-Derived Organoids

(A–C) LOH events at the *APC* locus that lead to loss of the wild-type allele in mice I, II, and III in (A), (B), and (C), respectively. Blue dots mark heterozygous alleles; red dots depict LOH. The entire length of chromosome 18 is depicted; liver and normal and tumor-derived organoids are compared. Further explanation of designations is given in the Figure 2 legend.

only then are there enough sequencing reads mapping to the human genome to allow distinguishing genomic deletions and duplications from noise. Analysis of all the organoids revealed only two CNAs, both of which were present in the same tumor-derived organoid. The first CNA resulted in the deletion of the telomeric 13 Mb of the q arm of chromosome 4 (Figure S1A), whereas the second CNA was a focal deletion of 0.23 Mb within the q arm of chromosome 18 (Figure S1B). The latter CNA targets the *Apc* gene, resulting in the deletion of its wild-type allele. Thus, this CNA is likely to have facilitated cancer progression. Analysis of the genes located within the deleted segment of chromosome 4 did not reveal the presence of genes with obvious links to cancer development.

Loss of Heterozygosity

As a final analysis of genomic instability, we monitored the presence of loss-of-heterozygosity (LOH) events, focusing especially on chromosome 18, which encompasses the *Apc* gene. The exome sequencing of genomic liver DNA from each mouse revealed, on average, 2,451 single-nucleotide variants (SNVs) per mouse, of which 87.4% were heterozygous and 12.6% were homozygous. The *Apc* locus was heterozygous in all normal organoids, with one allele bearing the nonsense Apc^{min} mutation and the other allele being wild-type. On the contrary, in all tumor-derived organoids—with the exception of organoids I-T1A and I-T1B, which originated from the same tumor—we identified LOH events at the *Apc* locus that led to loss of the wild-type allele. In 12 of 13 tumor-derived organoids, the LOH event involving *Apc* extended to the *Iws1* gene, which encodes an assembly factor for the RNA polymerase II (RNAPII) elongation complex (Diebold et al., 2010); whereas, in all the tumor-derived organoids from mouse III, the LOH events extended beyond the *Wdr7* locus (Figure 4).

Since adenoma development in $Apc^{min/+}$ mice requires the inactivation of both *Apc* alleles (Luongo et al., 1994), we examined more carefully the two tumor-derived organoids that did not exhibit LOH at the *Apc* locus. In one of these (I-T1A), we identified a 2-bp frameshift insertion, 175 nt downstream of the original Apc^{min} mutation (Table S3). This insertion is predicted to affect the Apc protein product. On the other hand, we did not identify mutations in the *Apc* locus in organoid I-T1B, although we cannot exclude events that can be easily missed by exome sequencing, such as, for example, the deletion of an entire exon.

DISCUSSION

While significant progress has been made in understanding the mechanisms leading to genomic instability in human cancers, many questions remain unanswered. One of these relates to the mechanisms by which SNSs are acquired in cancers. It is already clear that there are multiple signatures of SNSs in various cancers, thanks to recent studies describing as many as 30

distinct signatures in humans (Alexandrov et al., 2013; Helleday et al., 2014; Nik-Zainal et al., 2012). For some of these signatures, the underlying molecular mechanisms have been established or are being inferred. However, for other signatures, no clear mechanism is evident.

The most common SNS signature in human cancers, often referred to as signature 1, involves substitutions of C with T, especially in the context of CpG dinucleotides. Mechanistically, this involves deamination of methylated cytosines, leading to the formation of thymines, which may not be recognized as foreign and, therefore, not be efficiently repaired by base excision repair (Hendrich et al., 1999; Nikolaev et al., 2012). The prevailing concept in the field is that these SNSs are aging related (Alexandrov et al., 2013; Tomasetti et al., 2013; Tomasetti and Vogelstein, 2015; Vogelstein et al., 2013). According to this model, normal cells accumulate CpG-to-TpG substitutions at a constant rate over time; thus, any cancer cell that arises from a normal cell would contain all the substitutions present in the genome of the cell of origin. As a consequence, the number of signature 1 SNSs would be proportional to the age of the individual with cancer.

An assumption of the model described above is that the rate of accumulation of CpG-to-TpG mutations is the same in normal and precancerous/cancer cells. However, determining mutation rates in vivo is not trivial. We previously sequenced the exomes of early and late human colon adenomas and observed that the number of SNSs correlated with tumor size but not patient age (Nikolaev et al., 2012). From these observations, we proposed that the rate of acquisition of CpG-to-TpG transitions is higher in precancerous and cancer cells than in normal cells, as had been predicted by the mutator phenotype hypothesis (Bielas et al., 2006; Loeb, 2011). However, our previous study inferred mutation rates in normal cells from the analysis of the early adenomas rather than directly comparing normal cells to precancerous cells.

The DNA sequence analysis of organoids described here allows us to effectively interrogate the in vivo exomes of single normal and precancerous cells by expanding single stem cells in tissue culture as organoids. The same strategy has been used to identify point mutations in single normal intestinal stem cells from mice and humans (Behjati et al., 2014; Blokzijl et al., 2016). Considering that the proliferation rates of normal and cancer small intestinal cells are very similar, the rate of acquisition of SNSs appears to be almost 11 times higher in precancerous cells than in normal cells (Table S4). The actual rate may, in fact, be even higher, given that the tumors did not arise at the time of birth but rather at a later date, which means that the adenoma-associated SNSs arose within a shorter time window than the normal tissue-associated SNSs. The fact that organoids derived from the same tumor had a different set of SNSs further supports the argument that the SNSs were acquired after the transformation of normal cells into precancerous cells. Finally, it is unlikely that the mutations we observed were acquired during expansion of the organoids in tissue culture, as propagating the organoids for 3 additional months in vitro led to a small number of additional SNSs that could be distinguished from the SNSs acquired in vivo on the basis of lower allele frequencies and lack of a specific mutational signature. We conclude that precancerous cells—and, most likely, cancer cells—have a mutator phenotype as far as SNSs are concerned. We note, of course, that we cataloged SNSs in protein coding regions of the genome. While we expect that our conclusions will apply to the rest of the genome, future studies using genome-wide coverage will be needed to definitively address this point.

One of the culprits contributing to higher mutation rates for CpG-to-TpG substitutions in precancerous lesions might be DNA replication stress, which is prevalent in human precancerous lesions and cancers (Bartkova et al., 2005, 2006; Gorgoulis et al., 2005; Halazonetis et al., 2008). DNA replication stress leads to collapsed DNA replication forks and eventually to double-stranded breaks. These DNA lesions are repaired by break-induced replication (BIR), which has been associated with single-stranded DNA formation and elevated mutational rates (Costantino et al., 2014; Deem et al., 2011; Roumelioti et al., 2016; Sakofsky et al., 2014). Cytosines in CpG motifs are often methylated, and their deamination converts them to thymines. The resulting mismatches can serve as signals for efficient repair by the base excision repair machinery, but only in the context of double-stranded DNA (Hendrich et al., 1999). In the presence of single-stranded DNA, deaminated methyl-cytosines cannot be recognized as damaged bases. To compound the problem, the rate of cytosine deamination is about 100 times higher in single-stranded DNA than it is in double-stranded DNA (Lindahl and Nyberg, 1974; Lindahl, 1993). It will now be interesting to determine whether our findings can be extended to other tissue types and to human precancerous lesions and cancers.

EXPERIMENTAL PROCEDURES

Mice

The C57BL/6J-ApcMin/J mice were purchased from The Jackson Laboratory (Moser et al., 1990). All mice were kept on a 12-hr/12-hr light/dark cycle in an specific pathogen-free (SPF) room. The mice, all of which were males, were sacrificed at 4 months of age; all experiments were authorized by the Canton of Lausanne and were performed according to accepted guidelines for animal handling.

Organoid Preparation and Culture

Small-intestine tissue was isolated from C57BL/6J-ApcMin/J mice. The tissue was washed in cold PBS; healthy looking regions were separated from regions where tumors were present; each tumor was treated separately, and intestinal organoids were cultured as described previously (Sato et al., 2009).

Immunofluorescence

Organoids were removed from Matrigel using Corning Cell Recovery Solution and then were embedded in OCT (optimal cutting temperature) medium and sliced. Sections were fixed in 4% paraformaldehyde and stained using standard immunofluorescence techniques and commercially available antibody for γH2AX; nuclei were counterstained with DAPI.

DNA Extraction and Exome Sequencing

DNA was extracted and fragmented by sonication. The resultant fragments (~200 bp) were subjected to exome capture using the SureSelect Mouse All Exon Kit (Agilent Technologies), followed by preparation of paired-end libraries and sequencing on an Illumina HiSeq 2500 platform.

Sequence Analysis

The Burrows-Wheeler Alignment tool v.0.7.12 was used for the alignment of sequenced reads on the mouse reference genome NCBI Build GRCm38/mm10. The resultant files were processed using SAMtools v.1.3 in order to

perform bam transformation, sorting, removal of PCR duplicates, and indexing. To detect LOH events, we used the HaplotypeCaller algorithm of the GATK toolkit v.3.5.0 in order to call all the heterozygous SNS variants in liver and all the homozygous SNS variants in normal and tumor-derived organoids and then look for possible overlaps. The mutational spectra of detected somatic SNSs were examined using the SomaticSignature v.2.10.0 R package for the analysis of all the 96 possible trinucleotide changes. For the detection of CNAs, bam files were analyzed by VarScan2 v.2.2.4 using the recommended workflow. In order to detect somatic CNA events, we excluded CNAs that were present in the liver tissue of the mouse from which the organoids were prepared.

ACCESSION NUMBERS

The accession number for the FASTQ files reported in this paper is SRA: SRP102772.

SUPPLEMENTAL INFORMATION

Supplemental Information includes Supplemental Experimental Procedures, one figure, and four tables and can be found with this article online at http://dx.doi.org/10.1016/j.celrep.2017.05.051.

AUTHOR CONTRIBUTIONS

All authors conceived the study. N.L., P.O.-M., and I.K. planned and performed the experiments. V.S.D. and T.D.H. analyzed the sequencing data and performed the statistical analysis. N.L., V.S.D., P.O.-M., I.K., S.K.S., T.D.H., and J.H. proposed experiments, discussed the results, and contributed to the writing of the manuscript.

ACKNOWLEDGMENTS

The authors thank the Genetics and Genomics Platform of the University of Geneva (iGE3) for sequencing and Nicolas Roggli for help with figure preparation. This study was supported by funds from the Pictet Group Charitable Foundation to J.H. and T.D.H.

Received: February 28, 2017
Revised: April 11, 2017
Accepted: May 14, 2017
Published: June 13, 2017

REFERENCES

Alexandrov, L.B., Nik-Zainal, S., Wedge, D.C., Aparicio, S.A., Behjati, S., Biankin, A.V., Bignell, G.R., Bolli, N., Borg, A., Børresen-Dale, A.L., et al.; Australian Pancreatic Cancer Genome Initiative; ICGC Breast Cancer Consortium; ICGC MMML-Seq Consortium; ICGC PedBrain (2013). Signatures of mutational processes in human cancer. Nature *500*, 415–421.

Barker, N., Ridgway, R.A., van Es, J.H., van de Wetering, M., Begthel, H., van den Born, M., Danenberg, E., Clarke, A.R., Sansom, O.J., and Clevers, H. (2009). Crypt stem cells as the cells-of-origin of intestinal cancer. Nature *457*, 608–611.

Bartkova, J., Horejsí, Z., Koed, K., Krämer, A., Tort, F., Zieger, K., Guldberg, P., Sehested, M., Nesland, J.M., Lukas, C., et al. (2005). DNA damage response as a candidate anti-cancer barrier in early human tumorigenesis. Nature *434*, 864–870.

Bartkova, J., Rezaei, N., Liontos, M., Karakaidos, P., Kletsas, D., Issaeva, N., Vassiliou, L.V., Kolettas, E., Niforou, K., Zoumpourlis, V.C., et al. (2006). Oncogene-induced senescence is part of the tumorigenesis barrier imposed by DNA damage checkpoints. Nature *444*, 633–637.

Behjati, S., Huch, M., van Boxtel, R., Karthaus, W., Wedge, D.C., Tamuri, A.U., Martincorena, I., Petljak, M., Alexandrov, L.B., Gundem, G., et al. (2014). Genome sequencing of normal cells reveals developmental lineages and mutational processes. Nature *513*, 422–425.

Bielas, J.H., Loeb, K.R., Rubin, B.P., True, L.D., and Loeb, L.A. (2006). Human cancers express a mutator phenotype. Proc. Natl. Acad. Sci. USA *103*, 18238–18242.

Blokzijl, F., de Ligt, J., Jager, M., Sasselli, V., Roerink, S., Sasaki, N., Huch, M., Boymans, S., Kuijk, E., Prins, P., et al. (2016). Tissue-specific mutation accumulation in human adult stem cells during life. Nature *538*, 260–264.

Burrell, R.A., and Swanton, C. (2014). Tumour heterogeneity and the evolution of polyclonal drug resistance. Mol. Oncol. *8*, 1095–1111.

Burrell, R.A., McClelland, S.E., Endesfelder, D., Groth, P., Weller, M.C., Shaikh, N., Domingo, E., Kanu, N., Dewhurst, S.M., Gronroos, E., et al. (2013). Replication stress links structural and numerical cancer chromosomal instability. Nature *494*, 492–496.

The Cancer Genome Atlas Network (2012). Comprehensive molecular characterization of human colon and rectal cancer. Nature *487*, 330–337.

Costantino, L., Sotiriou, S.K., Rantala, J.K., Magin, S., Mladenov, E., Helleday, T., Haber, J.E., Iliakis, G., Kallioniemi, O.P., and Halazonetis, T.D. (2014). Break-induced replication repair of damaged forks induces genomic duplications in human cells. Science *343*, 88–91.

Deem, A., Keszthelyi, A., Blackgrove, T., Vayl, A., Coffey, B., Mathur, R., Chabes, A., and Malkova, A. (2011). Break-induced replication is highly inaccurate. PLoS Biol. *9*, e1000594.

Diebold, M.L., Koch, M., Loeliger, E., Cura, V., Winston, F., Cavarelli, J., and Romier, C. (2010). The structure of an Iws1/Spt6 complex reveals an interaction domain conserved in TFIIS, Elongin A and Med26. EMBO J. *29*, 3979–3991.

Drost, J., van Jaarsveld, R.H., Ponsioen, B., Zimberlin, C., van Boxtel, R., Buijs, A., Sachs, N., Overmeer, R.M., Offerhaus, G.J., Begthel, H., et al. (2015). Sequential cancer mutations in cultured human intestinal stem cells. Nature *521*, 43–47.

Fearon, E.R. (2011). Molecular genetics of colorectal cancer. Annu. Rev. Pathol. *6*, 479–507.

Fishel, R., Lescoe, M.K., Rao, M.R., Copeland, N.G., Jenkins, N.A., Garber, J., Kane, M., and Kolodner, R. (1993). The human mutator gene homolog MSH2 and its association with hereditary nonpolyposis colon cancer. Cell *75*, 1027–1038.

Gaspar, C., Cardoso, J., Franken, P., Molenaar, L., Morreau, H., Möslein, G., Sampson, J., Boer, J.M., de Menezes, R.X., and Fodde, R. (2008). Cross-species comparison of human and mouse intestinal polyps reveals conserved mechanisms in adenomatous polyposis coli (APC)-driven tumorigenesis. Am. J. Pathol. *172*, 1363–1380.

Gerlinger, M., Rowan, A.J., Horswell, S., Larkin, J., Endesfelder, D., Gronroos, E., Martinez, P., Matthews, N., Stewart, A., Tarpey, P., et al. (2012). Intratumor heterogeneity and branched evolution revealed by multiregion sequencing. N. Engl. J. Med. *366*, 883–892.

Gorgoulis, V.G., Vassiliou, L.V., Karakaidos, P., Zacharatos, P., Kotsinas, A., Liloglou, T., Venere, M., Ditullio, R.A., Jr., Kastrinakis, N.G., Levy, B., et al. (2005). Activation of the DNA damage checkpoint and genomic instability in human precancerous lesions. Nature *434*, 907–913.

Halazonetis, T.D., Gorgoulis, V.G., and Bartek, J. (2008). An oncogene-induced DNA damage model for cancer development. Science *319*, 1352–1355.

Halberg, R.B., Katzung, D.S., Hoff, P.D., Moser, A.R., Cole, C.E., Lubet, R.A., Donehower, L.A., Jacoby, R.F., and Dove, W.F. (2000). Tumorigenesis in the multiple intestinal neoplasia mouse: redundancy of negative regulators and specificity of modifiers. Proc. Natl. Acad. Sci. USA *97*, 3461–3466.

Helleday, T., Eshtad, S., and Nik-Zainal, S. (2014). Mechanisms underlying mutational signatures in human cancers. Nat. Rev. Genet. *15*, 585–598.

Hendrich, B., Hardeland, U., Ng, H.H., Jiricny, J., and Bird, A. (1999). The thymine glycosylase MBD4 can bind to the product of deamination at methylated CpG sites. Nature *401*, 301–304.

Lindahl, T. (1993). Instability and decay of the primary structure of DNA. Nature *362*, 709–715.

Lindahl, T., and Nyberg, B. (1974). Heat-induced deamination of cytosine residues in deoxyribonucleic acid. Biochemistry *13*, 3405–3410.

Loeb, L.A. (2011). Human cancers express mutator phenotypes: origin, consequences and targeting. Nat. Rev. Cancer *11*, 450–457.

Luongo, C., Moser, A.R., Gledhill, S., and Dove, W.F. (1994). Loss of Apc+ in intestinal adenomas from Min mice. Cancer Res. *54*, 5947–5952.

Moser, A.R., Pitot, H.C., and Dove, W.F. (1990). A dominant mutation that predisposes to multiple intestinal neoplasia in the mouse. Science *247*, 322–324.

Moser, A.R., Dove, W.F., Roth, K.A., and Gordon, J.I. (1992). The Min (multiple intestinal neoplasia) mutation: its effect on gut epithelial cell differentiation and interaction with a modifier system. J. Cell Biol. *116*, 1517–1526.

Moser, A.R., Luongo, C., Gould, K.A., McNeley, M.K., Shoemaker, A.R., and Dove, W.F. (1995). ApcMin: a mouse model for intestinal and mammary tumorigenesis. Eur. J. Cancer *31A*, 1061–1064.

Nassar, D., Latil, M., Boeckx, B., Lambrechts, D., and Blanpain, C. (2015). Genomic landscape of carcinogen-induced and genetically induced mouse skin squamous cell carcinoma. Nat. Med. *21*, 946–954.

Negrini, S., Gorgoulis, V.G., and Halazonetis, T.D. (2010). Genomic instability–an evolving hallmark of cancer. Nat. Rev. Mol. Cell Biol. *11*, 220–228.

Nik-Zainal, S., Alexandrov, L.B., Wedge, D.C., Van Loo, P., Greenman, C.D., Raine, K., Jones, D., Hinton, J., Marshall, J., Stebbings, L.A., et al.; Breast Cancer Working Group of the International Cancer Genome Consortium (2012). Mutational processes molding the genomes of 21 breast cancers. Cell *149*, 979–993.

Nikolaev, S.I., Sotiriou, S.K., Pateras, I.S., Santoni, F., Sougioultzis, S., Edgren, H., Almusa, H., Robyr, D., Guipponi, M., Saarela, J., et al. (2012). A single-nucleotide substitution mutator phenotype revealed by exome sequencing of human colon adenomas. Cancer Res. *72*, 6279–6289.

Roumelioti, F.M., Sotiriou, S.K., Katsini, V., Chiourea, M., Halazonetis, T.D., and Gagos, S. (2016). Alternative lengthening of human telomeres is a conservative DNA replication process with features of break-induced replication. EMBO Rep. *17*, 1731–1737.

Sakofsky, C.J., Roberts, S.A., Malc, E., Mieczkowski, P.A., Resnick, M.A., Gordenin, D.A., and Malkova, A. (2014). Break-induced replication is a source of mutation clusters underlying kataegis. Cell Rep. *7*, 1640–1648.

Sato, T., Vries, R.G., Snippert, H.J., van de Wetering, M., Barker, N., Stange, D.E., van Es, J.H., Abo, A., Kujala, P., Peters, P.J., and Clevers, H. (2009). Single Lgr5 stem cells build crypt-villus structures in vitro without a mesenchymal niche. Nature *459*, 262–265.

Sato, T., Stange, D.E., Ferrante, M., Vries, R.G., Van Es, J.H., Van den Brink, S., Van Houdt, W.J., Pronk, A., Van Gorp, J., Siersema, P.D., and Clevers, H. (2011). Long-term expansion of epithelial organoids from human colon, adenoma, adenocarcinoma, and Barrett's epithelium. Gastroenterology *141*, 1762–1772.

Schepers, A.G., Snippert, H.J., Stange, D.E., van den Born, M., van Es, J.H., van de Wetering, M., and Clevers, H. (2012). Lineage tracing reveals Lgr5+ stem cell activity in mouse intestinal adenomas. Science *337*, 730–735.

Sjöblom, T., Jones, S., Wood, L.D., Parsons, D.W., Lin, J., Barber, T.D., Mandelker, D., Leary, R.J., Ptak, J., Silliman, N., et al. (2006). The consensus coding sequences of human breast and colorectal cancers. Science *314*, 268–274.

Stratton, M.R. (2011). Exploring the genomes of cancer cells: progress and promise. Science *331*, 1553–1558.

Tomasetti, C., and Vogelstein, B. (2015). Cancer etiology. Variation in cancer risk among tissues can be explained by the number of stem cell divisions. Science *347*, 78–81.

Tomasetti, C., Vogelstein, B., and Parmigiani, G. (2013). Half or more of the somatic mutations in cancers of self-renewing tissues originate prior to tumor initiation. Proc. Natl. Acad. Sci. USA *110*, 1999–2004.

Vogelstein, B., Papadopoulos, N., Velculescu, V.E., Zhou, S., Diaz, L.A., Jr., and Kinzler, K.W. (2013). Cancer genome landscapes. Science *339*, 1546–1558.

Yamada, Y., and Mori, H. (2007). Multistep carcinogenesis of the colon in Apc(Min/+) mouse. Cancer Sci. *98*, 6–10.